Study of Optical and Electrochemical Properties of Solvent-Dependent Natural Dye Extracted from *Rivina humilis* L

Hasniah Aliah[1*], Ryan N. Iman[2], Sriwidati Sriwidati[1], Asti Sawitri[3],
Andhy Setiawan[4], Assa P.D. Putri[1], Fera Kurniawati[1]

1 Department of Physics, Faculty of Science and Technology, UIN Sunan Gunung Djati Bandung, Jl. A.H Nasution No. 105, Cibiru 40614, Indonesia

2 Department of Physics, College of Engineering and Physics, King Fahd University of Petroleum and Minerals, Academic Belt Road, Dhahran 31261, Saudi Arabia

3 Study Program of Physics, Faculty of Mathematics and Science, Universitas Halim Sanusi, Bandung, Jl. Garut No.2, Bandung, Jawa Barat 40271, Indonesia

4 Study Program of Physics, Faculty of Science and Mathematics, Universitas Pendidikan Indonesia, Jl. Dr. Setiabudhi No. 229 Bandung 40154, Indonesia

* Corresponding author's e-mail: hasniahaliah@uinsgd.ac.id

ABSTRACT

This work aimed to study the natural dye extracted from Indonesian wild plants (*Rivina humilis* L.) using different solvents. The natural dye was extracted using the maceration method. Three different solvents, namely, aquades, acetone, and ethanol 96%, were used to extract natural dye from *Rivina humilis* L fruit. The absorbance spectra of the extracted dye were recorded using Ultraviolet-Visible (UV-Vis) spectroscopy. The different spectra of betalain pigment revealed the dye extract's dependence on the solvent. The functional groups of the extracted dye were analyzed using Fourier transform infrared (FTIR) spectroscopy. The adherence of carbonyl and hydroxyl groups from FTIR spectra indicated that this dye could anchor to a semiconducting material, e.g., TiO_2 which was commonly used in dye-sensitized solar cells (DSSC). The electrochemical properties of the extracted pigments were studied through higher occupied molecular orbital (HOMO) and lower unoccupied molecular orbital (LUMO) energy levels. Based on the results, the best performance to construct DSSC was achieved by natural dye adsorption with aquades solvent.

Keywords: natural dye, betalain, *Rivina humilis L*, DSSC, HOMO, LUMO.

INTRODUCTION

The world's energy demands are increasing while fossil energy sources are dwindling, which is the main reason for using solar energy sources (Shah et al., 2023). Solar energy sources in tropical areas, such as Indonesia, have a high potential for development because they are abundant, environmentally friendly, and renewable. Electrical energy can be fulfilled by converting light into electricity based on the photoelectric principle of solar cell devices. For the first time, O'Regan and Gratzel discovered a low-cost photovoltaic cell known as dye-sensitized solar cells. This technology was constructed with transparent conductive substrates, dye, electrolyte, semiconductor, and counter electrode (O'regan & Grätzel, 1991). The dye acts as a photon catcher, and other components execute the trapped photons to obtain electrons. Sensitizers (dye) can be obtained from various sources, either synthetic or natural. Synthetic dyes such as ruthenium, osmium, and other metal complex-based dyes were reported as the most stable and effective for dye-sensitized solar cells (DSSC) (Dhonde et al., 2022; Huang et al., 2018). However, synthetic dyes have drawbacks in complex chemical processes, not environmentally friendly or toxic, limited availability, and expensive fabrication (Alkali et al., 2022; Mejica et al., 2022; Yadav et al., 2023). Therefore, we need

a sensitizer that is abundantly available, easy to extract, friendly to the environment, and simple and inexpensive to fabricate (Adedokun et al., 2021; Oladeji et al., 2022; Yadav et al., 2023).

Development of using natural dyes as sensitizers have been reported (Aliah et al., 2018; Erande et al., 2020; Najihah et al., 2022; Purushothamreddy et al., 2020). The natural dyes can be obtained from plants such as fruit, flowers, roots, and leaves (Abdel-latif et al., 2015; Al-Alwani et al., 2017; Madnasri & Ati, 2021; Prakash & Janarthanan, 2023) or algae and bacteria (Orona-Navar et al., 2021). Pigments that can be produced from plants include betalain (Guerrero-Rubio et al., 2020), anthocyanins (Obi et al., 2020), chlorophyll (Diantoro et al., 2019), etc. Betalain is one of the pigments that could produce high photo-current conversion. Betalain can be in terms of betaxanthin or betacyanin. Sinha et al. extracted betaxanthin from *Curcuma longa* with an ethanol solvent. They obtained a cell efficiency of 0.33% (Sinha et al., 2018). Purushothamreddy et al. extracted betacyanin from Prickly fruit with ethanol solvent. They achieved a cell efficiency of 0.5% (Purushothamreddy et al., 2020). Obi et al. achieved cell efficiency of 0.65% by extracting Prickly pear fruit with methanol/water (Obi et al., 2020). According to the literature, the type of solvent also affected the extracted dye, which can show better performance. It is due to the dye having different solubility that depends on their polarity, which influences the cell efficiency (Adedokun et al., 2018; Hemmatzadeh & Jamali, 2015; Obi et al., 2020). However, many of these studies concentrated on employing limited extraction solvents for certain natural pigments.

This study used the fruit of *Rivina humilis* L as a natural dye source. It is a wild plant that grows in colonies on black soil with a height of about 120 cm (M.I. Khan et al., 2011). A group of pigments known as betalain is discovered in plants in the order *Caryophyllales* (Gandía-Herrero et al., 2016). The two families of betalain are betaxanthins, which seem yellow-orange, and betacyanins, which comprise red-violet pigments (Strack et al., 2003). The *Rivina humilis* L. fruit was extracted with different solvents such as aquades, acetone, and ethanol 96%. The absorbance of the extracted dye and its electrochemical property were analyzed. The effect of three different solvents was studied for optimizing a low-cost dye-sensitized solar cell construction.

METHODOLOGY

Preparation of dyes

Rivina humilis L. fruit was obtained in West Java, Indonesia. The fruits were washed using deionized water and dried in the open air for 30 minutes. 15 grams of fruit were put into three glasses and pounded. Then, the glass containing the collision results was added with 15 mL of different solvents. Sample 1 used Aquades, Sample 2 used acetone, and Sample 3 used ethanol 96%. Each sample was stirred for 15 minutes using a stirrer. Afterward, the three samples were allowed to stand for 24 hours in dark conditions. After 24 hours, the three samples were filtered using filter paper (Whatman) to obtain pure dye from *Rivina humilis* fruit.

Fabrication of dye-coated TiO$_2$

Three pieces of FTO (Fluorine-Doped Tin Oxide) had been used as the substrates. The substrates were purchased from Sigma-Aldrich. The substrate's dimensions were 1.5×1.5 cm. They were cleaned for 10 minutes in each solvent with DI water, acetone, and ethanol 96%, respectively. Then, they were dried for 20 minutes in the open air. Titanium anatase paste was prepared by mixing 2 grams of Titanium dioxide powders (Titan Oxide anatase, Bratachem, PT. Brataco) with 6.5 mL of ethanol 96%. The mixture was stirred for 2 hours using a magnetic stirrer with 300 rpm. Afterward, the paste was put on the masked conductive side and squeezed one time in one direction. This technique is called screen printing (N et al., 2017). The TiO$_2$-coated substrate was then heated at 400 °C for 10 minutes using a furnace. The sample underwent preheating (below 400 °C) in the furnace because it needed 30 minutes to catch from room temperature to 400 °C. The temperature was kept at 400 °C for 10 minutes and let go down until room temperature. Next, the TiO$_2$-coated substrates were immersed in each dye solution for 24 hours. After immersion, dye-coated TiO$_2$ film was rinsed using ethanol 96% to remove the non-adsorbed dye and to clean the back side of the coated side. Finally, samples are ready to characterize.

Characterization of dye

Edinburgh Instruments DS5 UV-Vis Spectrophotometer was used to characterize the

absorption of the extracted dyes in the wavelength range of 300 nm to 800 nm. The functional groups of extracted dye were observed using Fourier transform infrared (FTIR) spectroscopy, Thermo Scientific Nicolet Is5. The energy level of the dye was examined using a potentiostat instrument, specifically the PGSTAT101 Metrohm AutoLab, which was connected to a computer containing the NOVA 1.11 software. An electrochemical measurement was conducted using three electrodes cell configuration. The working electrode (WE) consisted of a carbon paste electrode, the counter electrode (CE) utilized a Pt-wire, and the reference electrode (RE) employed an Ag/AgCl electrode. The samples were measured under the iodide/triode solution as an electrolyte. The electrolyte was made from Iodine and Potassium Iodide and then mixed using PEG 400 solvent. Figure 1 illustrates the cyclic voltammetry (CV) measurement set.

RESULTS AND DISCUSSION

Absorbance spectra analysis

The dye solutions are depicted in Figure 2. Various solvents produce different colors on the extract due to the various pigment components extracted (Adedokun et al., 2018). The dye slightly loses color when using organic solvents (acetone or ethanol).The absorbance spectra of the extracted dye with various solvents were examined using UV-Vis spectroscopy. The spectra were recorded at 300–800 nm wavelengths. Using solvent variations is intended to determine the optimization of the dye synthesis in achieving the highest light absorption. The absorbance examination results of dye extraction from *Rivina*

humilis L are depicted in Figure 3. It reveals that each dye solution absorbs the light at a different spectrum. Dye with aquades solvent has two absorption peaks, one main peak at 453 nm and one shoulder peak at 532 nm wavelengths. The peak at 453 nm corresponds to an orange band, while a peak at 532 nm corresponds to a red-violet band. Both peaks are attributed to the betalain component (Singh & Shukla, 2022) on the extracted dye with aquades solvent. The spectrum of the dye solution with acetone solvent appears a broad peak in the range of 416–505 nm. In addition, the peak of the dye solution with ethanol solvent appears at two wavelengths. The one main peak is at 450 nm, and the other at 479 nm corresponds to an orange band.

The absorption curve of the dye extract from *Rivina humilis* L is similar to the curve for the absorption area of betalain in general (Dias et al., 2020). The slight difference in the absorption spectra between the three dye solutions is due to using different solvents, leading to other photosynthetic properties (Biswas et al., 2013). This confirms that dye extracted with aquades has pigment properties of betaxanthins (453 nm) (Dias et al., 2020; M.I. Khan & Giridhar, 2015; Polturak & Aharoni, 2018) and betacyanin (532 nm) (Isah et al., 2015). Dye with acetone has pigment properties of betaxanthins (416–505 nm) (M.I. Khan & Giridhar, 2015; Polturak & Aharoni, 2018). In addition, a dye extracted with ethanol produces betaxanthin pigments. Betacyanin corresponds to red-purple, while betaxanthins correspond to yellow (Dumbravă et al., 2012; Gandía-Herrero et al., 2016). Based on the spectra above, all samples have spectra in the visible light region, and they are suitable for DSSC application (M.I.
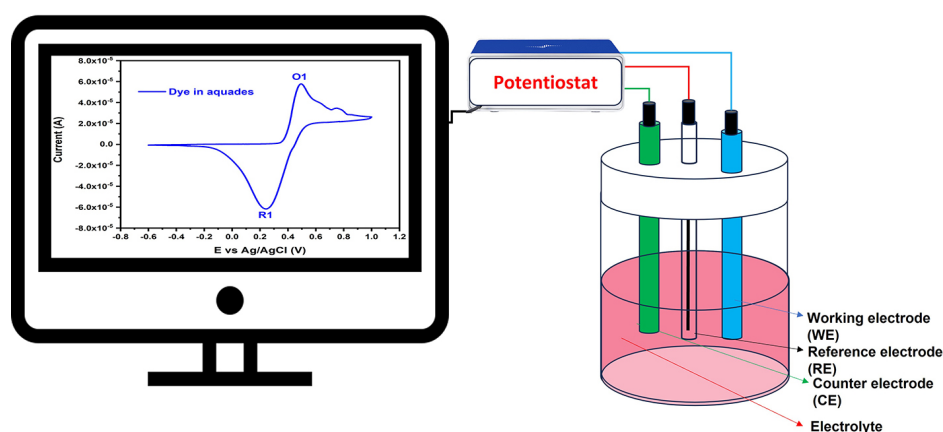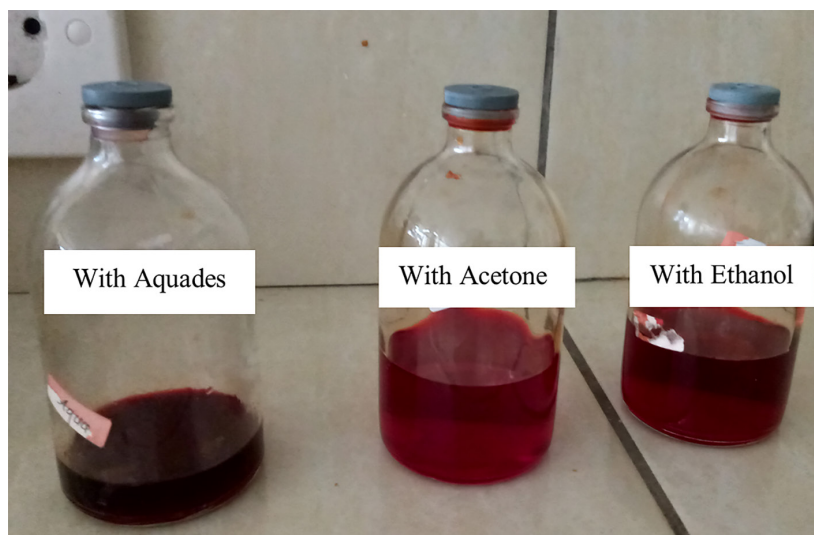

Figure 1. Schematic CV measurements

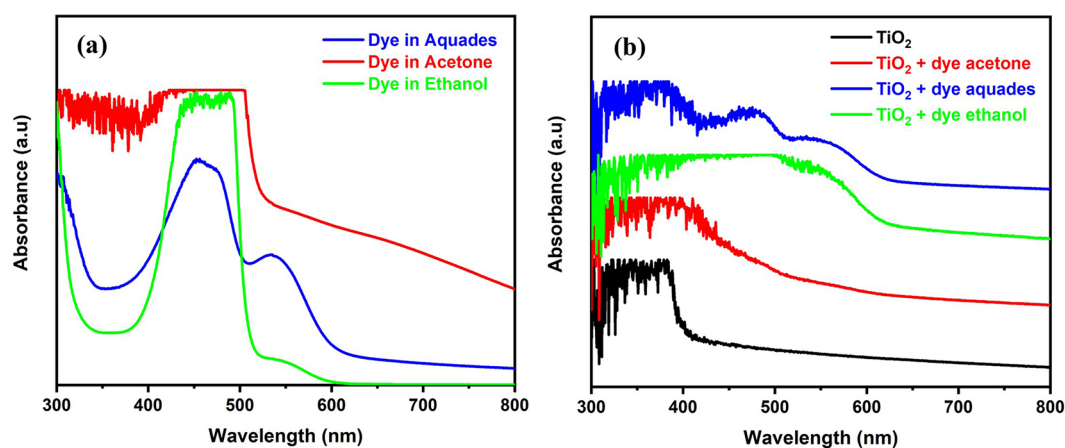**Figure 2.** The dye solutions of *Rivina humilis* L.

Figure 3. Absorbance spectra of (a) dye solution, (b) dye-adsorbed TiO$_2$ in different solvents

Khan et al., 2011; Prakash & Janarthanan, 2023; Srivastava et al., 2022).

Characteristics of dye-adsorbed TiO$_2$ are also studied to know their optical properties, as shown in Figure 3b. The pure TiO$_2$ spectrum pattern aligns with the UV-Vis spectrum of TiO$_2$ anatase observed by ref. (Haque et al., 2017). This means the fabricated pure TiO$_2$ film may have an anatase phase. As reported by Haque et al., the TiO$_2$ anatase has a bit narrower spectrum compared to TiO$_2$ rutile (Haque et al., 2017). The absorption spectra of the dye-adsorbed TiO$_2$ films indicate a noticeable increase in overall absorbance, as evidenced by the widening of peaks. Furthermore, it was found that the peaks exhibited a slight shift. The observed shifts and amplification in the absorbance can be attributed to two potential factors. First, incorporating carbonyl groups from the dye into TiO$_2$ in the dye/TiO$_2$ composite formation

results in a Ti-O-C bond, which can generate novel defect states and facilitate the introduction of oxygen atoms. The incorporation of an extra oxygen atom has the potential to enhance the efficiency of light harvesting. Enhancing the efficiency of light harvesting is expected to influence the performance of the DSSC positively. Second, after immersion of TiO$_2$-based films in the dye solution, a reduction in the π^* energy level delocalization is observed. This phenomenon corresponds to the binding of the carboxyl group in the extracted dye with the Ti^{4+} ion. The mechanisms mentioned earlier cause a shift in the absorbance peaks and an increase in the intensity of absorption (Ananth et al., 2014; Younas & Gondal, 2022).

The band gap energy value can optically be found using Tauc's plot method (Kumara et al., 2013). The plot method developed by Tauc is based on the relationship between the light energy

represented by the quantity $(\alpha h\nu)^2$ and the abscissa $h\nu$ described in the ordinate position. This relationship is then extrapolated to the linear region of the absorbance, ultimately reaching zero. Then it will be obtained an absorbance coefficient often denoted by α. The following equation (Eq. 1) can be used to figure out the bandgap energy (E_g) (A.A. Khan et al., 2022).

$$(\alpha h\nu)^{1/\gamma} = c(h\nu - E_g) \qquad (1)$$

where: α – coefficient of absorbance, c – a constant, ν –the frequency of the photon, h – the Planck constant, E_g –the band gap energy, γ – factor corresponds to the electron transition type, representing direct band gaps for $\gamma = 1/2$ and an indirect band gap for $\gamma = 2$ (Makuła et al., 2018).

The Tauc plot extrapolation results are shown in Figure 4. It reveals that the band gap energy values of dye-aquades, dye-acetone, and dye-ethanol at 2.08 eV, 2.34 eV, and 2.45 eV, successively, attributed to their absorption peak around 453–532 nm corresponding to betaxanthin and betacyanin (Dumbravă et al., 2012; Shah et al., 2023). Meanwhile, the band gap energy of pristine-TiO_2, dye (aquades)/TiO_2, dye (acetone)/TiO_2, and dye (ethanol)/TiO_2 are found at 3.1 eV, 1.76 eV, 1.98 eV, and 1.79 eV, successively (Fig. 4b). The band gap energy gets smaller after dye adsorption, which is due to the slight shifting in the spectra, as can be seen in Figure 3b. These shifts have two reasons, as mentioned above: (1) formation of Ti-O-C bond and (2) delocalization π^* energy level which is because of the bonding of carboxylate group in the dye with the Ti^{4+} ion (Younas & Gondal, 2022). As

reported, the band gap energy value affected the solar cell efficiency. The smaller band gap energy leads to the highest photo conversion efficiency due to the electron's ease of transfer (Elmorsy et al., 2023; Nan et al., 2017). Among all samples, the dye (aquades)-adsorbed TiO_2 is the most optimum configuration for DSSC application.

Fourier transform infrared spectra analysis

In addition to possessing a high degree of optical absorption, an essential criterion for an effective photosensitizer is the presence of chemical bonds within the dye pigment that readily anchor to the surface of the semiconductor. Figure 5 reveals FTIR spectra of extracted dyes. It was conducted to understand the chemical bonds better and identify the specific functional groups adhering to *Rivina humilis L*'s dye extract. The x-axis of the graph displays the wavelengths corresponding to the major absorbance peaks. Primary functional groups, particularly O-H (hydroxyl) and C=O (carbonyl) functional groups, were evident in all samples. These functional groups play an essential role in the adsorption and surface bonding to TiO_2 (A.A. Khan et al., 2022; Shah et al., 2023).

A prominent and wide absorption peak was detected at a wavenumber of 3366 cm^{-1}. The observed phenomenon can be assigned to the hydroxyl OH bonding (Patni et al., 2020; Purushothamreddy et al., 2020; Shah et al., 2023). The observed peak at 2925 cm^{-1} and 2854 cm^{-1} are attributed to aliphatic C–H bending vibration (Patni et al., 2020; Purushothamreddy et al., 2020; Shah et al., 2023). The peak of carbonyl C=O vibration was found at 1746 cm^{-1} (Purushothamreddy et al., 2020). The
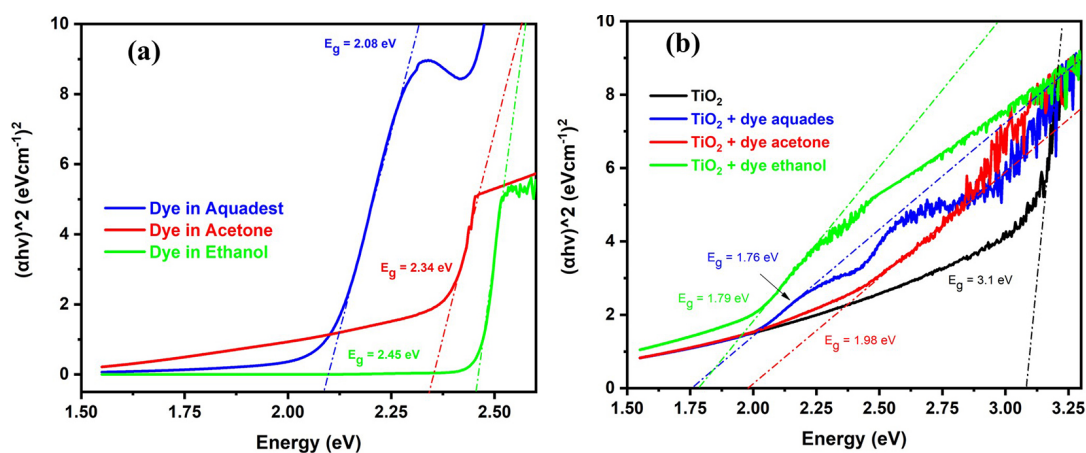

Figure 4. Tauc plot photon energy determination of (a) dye extracted with different solvents and (d) dye-adsorbed TiO_2 films
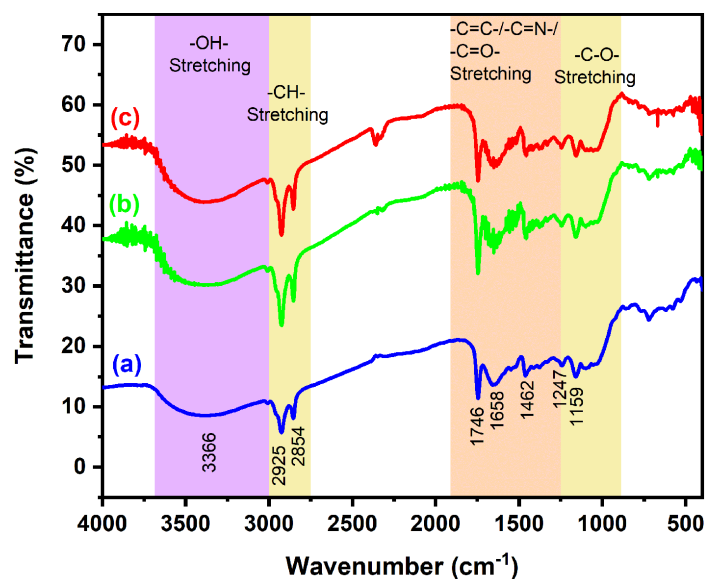
Figure 5. Fourier transforms infrared spectroscopy spectra of extracted dye with different solvents

C=N vibration was found at 1658 cm⁻¹ (Shah et al., 2023). The aromatic C=C bond is found at 1462 cm⁻¹ wavenumber (Purushothamreddy et al., 2020). The stretching vibrations are found at 1247 cm⁻¹ and 1159 cm⁻¹ assigned to C-O bonding (Shah et al., 2023). All stretching vibration peaks were assigned to the betalain family pigment, especially betacyanin, and betaxanthin (Patni et al., 2020; Purushothamreddy et al., 2020; Shah et al., 2023). The FTIR results of the extracted dyes from *Rivina humilis L* with various solvents reveal no distinct peaks. Therefore, it can be concluded that no additional chemical reactions occur in the dye. Different solvents, like aquades, acetone, and ethanol, affect only the absorption intensity, as seen in their intensity. The order of their absorption intensity is aquades > ethanol > acetone.

Electrochemical analysis

In DSSC, the creation of photo-current is dependent on the transfer of electrons from the dye to the semiconducting layer's conduction band. The electron transfer process needs a LUMO level of the donor that is more positive than the acceptor. Conversely, the transfer of holes from an acceptor to a donor needs a HOMO level of the donor (dye) to be more negative than the acceptor. This will decrease the recombination of the semiconductor layer interface, thereby improving the stability of the dye employed in DSSCs. HOMO corresponds to the quantity of energy required to generate the electrons from molecules,

commonly referred to as oxidation. The LUMO refers to the minimum energy necessary for the electron injection into a molecule, corresponding to a reduction process (Sinha et al., 2018).

Electrochemical characteristics of the extracted dyes are studied with Cyclic Voltammetry (CV). This characterization was conducted to determine the oxidation-reduction reaction and examine the ability of the extracted dyes to transfer the electrons from the LUMO state of the dye to the conduction band (CB) of TiO₂. Fig. 6 depicts the voltammogram curve obtained through scanning within a potential range of +1.0 V to -0.6 V, using a scan rate of 100 mV/s. Due to various solvents, the dyes exhibit different electrochemical characteristics with irreversible reduction (R1) and oxidation (O1). The LUMO and HOMO are calculated using Eq. 2 and 3 (Sinha et al., 2018).

$$E_{HOMO} = -e(E_{ox} + 4.4)eV \qquad (2)$$

$$E_{LUMO} = -e(E_{red} + 4.4)eV \qquad (3)$$

where: E_{ox} – the oxidation potential peak, E_{red} – the peak of reduction potential.

This value determines how electrons move, channeling the received photons and injecting them into TiO₂ as a collecting material. Table 1 summarizes the LUMO and HOMO energy levels of each dye in terms of vacuum energy level. The LUMO of the extracted dyes must be more positive than the TiO₂ CB for electron injection to work well (Najm et al., 2023; Sharma et al., 2023; Sinha et al., 2018). The HOMO of the dye
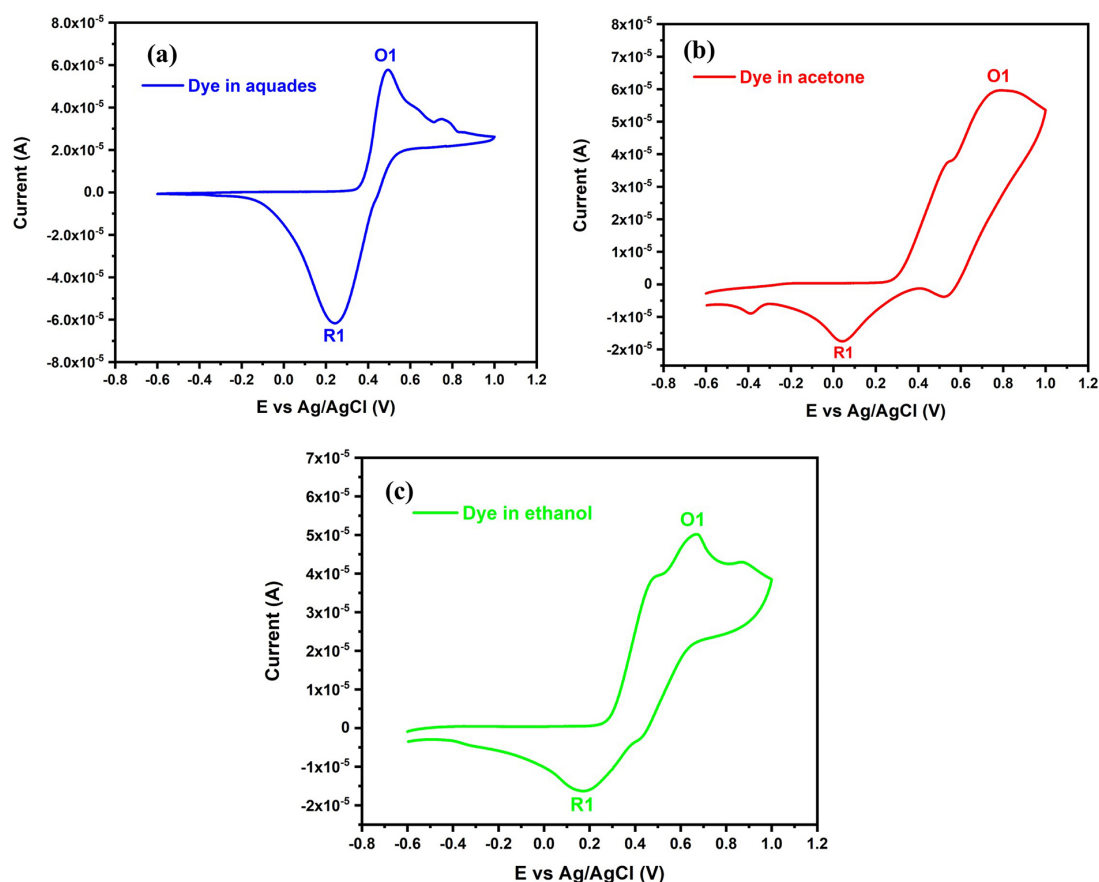
Figure 6. Cyclic voltammogram of the extracted dye with (a) aquades, (b) acetone, and (c) ethanol

Table 1. Summary of the calculated energy levels of the extracted dyes. The conduction and valence band values of TiO_2 were adapted from the reference [47]

No.	Sample	E_{ox} (V)	E_{red} (V)	LUMO (eV)	HOMO (eV)	Ref.
1.	Dye in Aquades	0.49	0.24	-4.64	-4.89	This work
2.	Dye in Acetone	0.66	0.17	-4.57	-5.06	This work
3.	Dye in Ethanol	0.76	0.04	-4.44	-5.16	This work
4.	TiO_2	-	-	-5.11 (CB)	-8.50 (VB)	[47]

Note: *CB – conduction band, VB – valence band.

must possess a more negative value than the energy level of the electrolyte to attain an efficient dye regeneration (Sharma et al., 2023; Sinha et al., 2018). The LUMO levels of each dye were found at -4.64 eV, -4.57 eV, and -4.44 eV for dye extract with aquades, acetone, and ethanol, respectively. In addition, the HOMO level of each dye was -4.89 eV, -5.06 eV, and -5.16 eV for extracted dyes with aquades, acetone, and ethanol solvents, respectively. It is evident that the LUMO energy levels of the extracted dyes exhibit a significant positive energy difference compared to the TiO_2 CB (-5.11 eV) at a vacuum level (Sung et al., 2020). The HOMO levels of dyes indicate negative values compared to the electrolyte's energy level (-4.85 eV) (Güzel

et al., 2018; Sung et al., 2020). This property enables the effective regeneration of oxidized dyes via electrolytes. Therefore, the process of injecting electrons is energetically advantageous.

CONCLUSIONS

This study aimed to discover the promising dyes which can be used in DSSC for high efficiency. The absorption of a single natural dye with different solvents has been reported in this work. The dyes have absorption spectra in the visible light region. The UV-Vis spectroscopy confirmed betaxanthin and betacyanin adhere in

the extracted dye with aquades solvent, while dye extracted with ethanol or acetone produces betaxanthin only. The FTIR spectroscopy confirmed the carbonyl and hydroxyl groups on the dyes. These functional groups anchored the dye with the TiO_2 surface, making higher light absorption. The lowest band gap of the dye (aquades) anchored TiO_2 leads to the easiness of the electron to transfer. The energy level of the dye revealed that it matched with TiO_2 CB and electrolyte energy levels. Therefore, this promising dye is suitable for high absorption in harvesting light. The dye (aquades)-adsorbed TiO_2 is the optimum configuration for DSSC application.

Acknowledgments

REFERENCES

1. Abdel-latif, M.S., Abuiriban, M.B., & El-agez, T.M. 2015. Dye-Sensitized Solar Cells Using Dyes Extracted From Flowers, Leaves, Parks, and Roots of Three Trees. January, 3–8.

2. Adedokun, O., Adedeji, O.L., Bello, I.T., Awodele, M.K., Awodugba, A.O. 2021. Fruit peels pigment extracts as a photosensitizer in ZnO-based Dye-Sensitized Solar Cells. Chemical Physics Impact, 3, 100039.

3. Adedokun, O., Sanusi, Y.K., Awodugba, A.O. 2018. Solvent dependent natural dye extraction and its sensitization effect for dye sensitized solar cells. Optik, 174, 497–507.

4. Al-Alwani, M.A.M., Ludin, N.A., Mohamad, A.B., Kadhum, A.A.H., Sopian, K. 2017. Extraction, preparation and application of pigments from Cordyline fruticosa and Hylocereus polyrhizus as sensitizers for dye-sensitized solar cells. Spectrochimica Acta - Part A: Molecular and Biomolecular Spectroscopy, 179, 23–31. https://doi.org/10.1016/j.saa.2017.02.026.

5. Aliah, H., Bernando, B., Puspitasari, F., Setiawan, A., Pitriana, P., Nuryadin, B.W., Ramdhani, M.A. 2018. Dye Sensitized Solar Cells (DSSC) Performance Reviewed from the Composition of Titanium Dioxide (TiO_2)/ Zinc Oxide (ZnO). IOP Conference Series: Materials Science and Engineering Paper, 288, 012070.

6. Alkali, B., Yerima, B.J., Ahmed, A.D., Ezike, S.C. 2022. Suppressed Charge Recombination Aided Co-Sensitization in Dye-Sensitized Solar Cells-Based Natural plant Extracts. Optik, 170072.

7. Ananth, S., Vivek, P., Arumanayagam, T., Murugakoothan, P. 2014. Natural dye extract of lawsonia inermis seed as photo sensitizer for titanium dioxide based dye sensitized solar cells. Spectrochimica Acta Part A: Molecular and Biomolecular Spectroscopy, 128, 420–426. https://doi.org/10.1016/j.saa.2014.02.169

8. Biswas, M., Dey, S., Sen, R. 2013. Betalains from Amaranthus tricolor L. Journal of Pharmacology and Phytochemistry, 1, 87–95.

9. Dhonde, M., Sahu, K., Das, M., Yadav, A., Ghosh, P., Murty, V.V.S. 2022. Review—Recent Advancements in Dye-Sensitized Solar Cells; From Photoelectrode to Counter Electrode. Journal of The Electrochemical Society, 169(6), 066507. https://doi.org/10.1149/1945-7111/ac741f

10. Diantoro, M., Maftuha, D., Suprayogi, T., Iqbal, M. R., Solehudin, Mufti, N., Taufiq, A., Hidayat, A., Suryana, R., Hidayat, R. 2019. Performance of Pterocarpus Indicus Willd Leaf Extract as Natural Dye TiO_2-Dye/ITO DSSC. Materials Today: Proceedings, 17, 1268–1276.

11. Dias, S., Castanheira, E.M.S., Gil Fortes, A., Pereira, D.M., Sameiro, M. 2020. Natural pigments of anthocyanin and betalain for coloring soy-based yogurt alternative. Foods, 9(6), 1–13. https://doi.org/10.3390/foods9060771

12. Dumbravă, A., Enache, I., Oprea, C.I., Georgescu, A., Gîrţu, M.A. 2012. Toward a more efficient utilisation of betalains as pigments for dye-sensitized solar celss. Digest Journal of Nanomaterials & Biostructures (DJNB), 7(1).

13. Elmorsy, M.R., Badawy, S.A., Abdel-Latif, E., Assiri, M.A., Ali, T.E. 2023. Significant improvement of dye-sensitized solar cell performance using low-band-gap chromophores based on triphenylamine and carbazole as strong donors. Dyes and Pigments, 214, 111206. https://doi.org/10.1016/j.dyepig.2023.111206

14. Erande, K.B., Hawaldar, P.Y., Suryawanshi, S.R., Babar, B.M., Mohite, A.A., Shelke, H.D., Nipane, S.V., Pawar, U.T. 2020. Extraction of natural dye (specifically anthocyanin) from pomegranate fruit source and their subsequent use in dssc. Materials Today: Proceedings, 43(40), 2716–2720. https://doi.org/10.1016/j.matpr.2020.06.357

15. Gandía-Herrero, F., Escribano, J., García-Carmona, F. 2016. Biological activities of plant pigments betalains. Critical Reviews in Food Science and Nutrition, 56(6), 937–945.

16. Guerrero-Rubio, M.A., Escribano, J., García-Carmona, F., Gandía-Herrero, F. 2020. Light Emission in Betalains: From Fluorescent Flowers to Biotechnological Applications. Trends in Plant Science, 25(2), 159–175. https://doi.org/10.1016/j.tplants.2019.11.001

17. Güzel, E., Arslan, B.S., Durmaz, V., Cesur, M., Tutar, Ö.F., Sarı, T., İşleyen, M., Nebioğlu, M., Şişman,

İ. 2018. Photovoltaic performance and photostability of anthocyanins, isoquinoline alkaloids and betalains as natural sensitizers for DSSCs. Solar Energy, 173, 34–41.

18. Haque, F.Z., Nandanwar, R., Singh, P. 2017. Evaluating photodegradation properties of anatase and rutile TiO$_2$ nanoparticles for organic compounds. Optik, 128, 191–200.

19. Hemmatzadeh, R., Jamali, A. 2015. Enhancing the optical absorption of anthocyanins for dye-sensitized solar cells. Journal of Renewable and Sustainable Energy, 7(1).

20. Huang, Y., Chen, W.-C., Zhang, X.-X., Ghadari, R., Fang, X.-Q., Yu, T., Kong, F.-T. 2018. Ruthenium complexes as sensitizers with phenyl-based bipyridine anchoring ligands for efficient dye-sensitized solar cells. Journal of Materials Chemistry C, 6(35), 9445–9452. https://doi.org/10.1039/C8TC03288B.

21. Isah, K.U., Ahmadu, U., Idris, A., Kimpa, M.I., Uno, U.E., Ndamitso, M.M., Alu, N. 2015. Betalain pigments as natural photosensitizers for dye-sensitized solar cells: The effect of dye pH on the photoelectric parameters. In Materials for Renewable and Sustainable Energy, 4(1), 5–9. https://doi.org/10.1007/s40243-014-0039-0

22. Khan, A.A., Adilah, M.Y.S., Mamat, M.H., Yahaya, S.Z., Setumin, S., Ibrahim, M.N., Daud, K., Abdullah, M.H. 2022. Magnesium sulfate as a potential dye additive for chlorophyll-based organic sensitiser of the dye-sensitised solar cell (DSSC). Spectrochimica Acta Part A: Molecular and Biomolecular Spectroscopy, 274, 121140.

23. Khan, M.I., Denny Joseph, K.M., Muralidhara, M., Ramesh, H.P., Giridhar, P., Ravishankar, G. A. 2011. Acute, subacute and subchronic safety assessment of betalains rich *Rivina humilis* L. berry juice in rats. Food and Chemical Toxicology, 49(12), 3154–3157. https://doi.org/10.1016/j.fct.2011.08.022

24. Khan, M.I., Giridhar, P. 2015. Plant betalains: Chemistry and biochemistry. Phytochemistry, 117, 267–295. https://doi.org/10.1016/j.phytochem.2015.06.008

25. Kumara, N.T.R.N., Ekanayake, P., Lim, A., Iskandar, M., Ming, L.C. 2013. Study of the enhancement of cell performance of dye sensitized solar cells sensitized with nephelium lappaceum (F: Sapindaceae). Journal of Solar Energy Engineering, Transactions of the ASME, 135(3), 1–6. https://doi.org/10.1115/1.4023877

26. Madnasri, S., Ati, L. 2021. Organic Solar Cell Performance of Musa acuminata bracts Extract by Microwave Irradiation Treatment. International Journal of Energy Research, 45(3), 4214–4223. https://doi.org/10.1002/er.6085

27. Makuła, P., Pacia, M., Macyk, W. 2018. How to correctly determine the band gap energy of modified semiconductor photocatalysts based on UV–Vis spectra. In The journal of physical chemistry letters, 9(23), 6814–6817. ACS Publications.

28. Mejica, G.F.C., Unpaprom, Y., Balakrishnan, D., Dussadee, N., Buochareon, S., Ramaraj, R. 2022. Anthocyanin pigment-based dye-sensitized solar cells with improved pH-dependent photovoltaic properties. Sustainable Energy Technologies and Assessments, 51, 101971.

29. Nurida A., Chintia A., Sakkyananda S., Aprilia A., Susilawati T., Mulyana C., Lusi Safriani L. 2017. Fabrikasi Sel Surya Tersensitasi Dye Dengan ZnO Nanorod Sebagai Fotoanoda dan Material Spiro Sebagai Hole Transport Material (HTM). Jurnal Ilmu Dan Inovasi Fisika, 1, 79–85.

30. Najihah, M.Z., Noor, I.M., Winie, T. 2022. Long-run performance of dye-sensitized solar cell using natural dye extracted from Costus woodsonii leaves. Optical Materials, 123, 111915.

31. Najm, A.S., Alwash, S.A., Sulaiman, N.H., Chowdhury, M.S., Techato, K. 2023. N719 dye as a sensitizer for dye-sensitized solar cells (DSSCs): A review of its functions and certain rudimentary principles. Environmental Progress & Sustainable Energy, 42(1), e13955.

32. Nan, H., Shen, H.-P., Wang, G., Xie, S.-D., Yang, G.-J., Lin, H. 2017. Studies on the optical and photoelectric properties of anthocyanin and chlorophyll as natural co-sensitizers in dye sensitized solar cell. Optical Materials, 73, 172–178.

33. O'regan, B., Grätzel, M. 1991. A low-cost, high-efficiency solar cell based on dye-sensitized colloidal TiO2 films. Nature, 353(6346), 737–740.

34. Obi, K., Frolova, L., Fuierer, P. 2020. Preparation and performance of prickly pear (*Opuntia phaeacantha*) and mulberry (*Morus rubra*) dye-sensitized solar cells. Solar Energy, 208, 312–320.

35. Oladeji, O.S., Ikhile, M.I., Mamo, M., Ndinteh, D.T., Ndungu, P.G. 2022. Extraction, characterization and energy investigation of Garcinia kola, Cola Nitida and Cola Accuminata for efficient light absorption in dye-sensitized solar cells. Solar Energy, 244, 386–400.

36. Orona-Navar, A., Aguilar-Hernández, I., Nigam, K.D.P., Cerdán-Pasarán, A., Ornelas-Soto, N. 2021. Alternative sources of natural pigments for dye-sensitized solar cells: Algae, cyanobacteria, bacteria, archaea and fungi. Journal of Biotechnology, 332, 29–53.

37. Patni, N., Pillai, S.G., Sharma, P. 2020. Effect of using betalain, anthocyanin and chlorophyll dyes together as a sensitizer on enhancing the efficiency of dye-sensitized solar cell. International Journal of Energy Research, 44(13), 10846–10859.

38. Polturak, G., Aharoni, A. 2018. La Vie en Rose: Biosynthesis, Sources, and Applications of Betalain Pigments. Molecular Plant, 11(1), 7–22.

39. Prakash, P., Janarthanan, B. 2023. Enhancement of

sensitization and electron transfer by kumkum dye in dye-sensitized solar cell applications. Optik, 287, 171093. https://doi.org/https://doi.org/10.1016/j.ijleo.2023.171093

40. Purushothamreddy, N., Dileep, R.K., Veerappan, G., Kovendhan, M., Joseph, D.P. 2020. Prickly pear fruit extract as photosensitizer for dye-sensitized solar cell. Spectrochimica Acta Part A: Molecular and Biomolecular Spectroscopy, 228, 117686.

41. Shah, W., Faraz, S.M., Awan, Z.H. 2023. Photovoltaic properties and impedance spectroscopy of dye sensitized solar cells co-sensitized by natural dyes. Physica B: Condensed Matter, 654, 414716.

42. Sharma, G., Singh, V., Dolia, S.N., Jain, I.P., Jain, P.K., Lal, C. 2023. Present status of metal-free photosensitizers for dye-sensitized solar cells. Materials Today: Proceedings. https://doi.org/10.1016/j.matpr.2023.02.179

43. Singh, P.K., Shukla, V.K. 2022. Widening spectral range of absorption using natural dyes: Applications in dye sensitized solar cell. Materials Today: Proceedings, 49, 3235–3238.

44. Sinha, D., De, D., Ayaz, A. 2018. Performance and stability analysis of curcumin dye as a photo sensitizer used in nanostructured ZnO based DSSC. Spectrochimica Acta - Part A: Molecular and Biomolecular Spectroscopy, 193, 467–474. https://doi.org/10.1016/j.saa.2017.12.058

45. Srivastava, A., Singh Chauhan, B., Chand Yadav, S., Kumar Tiwari, M., Akash Kumar Satrughna, J., Kanwade, A., Bala, K., Shirage, P.M. 2022. Performance of dye-sensitized solar cells by utilizing Codiaeum Variegatum Leaf and Delonix Regia Flower as natural sensitizers. Chemical Physics Letters, 807, 140087. /https://doi.org/10.1016/j.cplett.2022.140087.

46. Strack, D., Vogt, T., Schliemann, W. 2003. Recent advances in betalain research. Phytochemistry, 62(3), 247–269.

47. Sung, H.K., Lee, Y., Kim, W.H., Lee, S.-J., Sung, S.-J., Kim, D.-H., Han, Y.S. 2020. Enhanced power conversion efficiency of dye-sensitized solar cells by band edge shift of TiO_2 photoanode. Molecules, 25(7). https://doi.org/10.3390/molecules25071502

48. Yadav, S.C., Tiwari, M.K., Kanwade, A., Lee, H., Ogura, A., Shirage, P.M. 2023. Butea monosperma, crown of thorns, red lantana camara and royal poinciana flowers extract as natural dyes for dye sensitized solar cells with improved efficiency. Electrochimica Acta, 441, 141793.

49. Younas, M., Gondal, M.A. 2022. Economical and efficient dye sensitized solar cells using single wall carbon nanotube-titanium dioxide nanocomposites as photoanode and SWCNT as Pt-free counter electrode. Solar Energy, 245, 37–45.